

Effect of chondroitin sulfate proteoglycans on neuronal cell adhesion, spreading and neurite growth in culture

Jingyu Jin^{1,†}, Sharada Tilve^{2,†}, Zhonghai Huang¹, Libing Zhou¹, Herbert M. Geller², Panpan Yu^{1,*}

1 Guangdong-Hongkong-Macau Institute of CNS Regeneration; Ministry of Education Joint International Research Laboratory of CNS Regeneration, Jinan University, Guangzhou, Guangdong Province, China

2 Laboratory of Developmental Neurobiology, Cell Biology and Physiology Center, National Heart, Lung, and Blood Institute, National Institutes of Health, Bethesda, MD, USA

Funding: This work was supported by the National Natural Science Foundation of China, No. 81601066; the Natural Science Foundation of Guangdong Province of China, No. 2017A030313103 and 2016A030313096; a grant from the Program of Introducing Talents of Discipline to Universities, No. B14036; the Fundamental Research Funds for the Central Universities, No. 21616340; and the Division of Intramural Research of the National Heart, Lung, and Blood Institute of National Institutes of Health.

Abstract

As one major component of extracellular matrix (ECM) in the central nervous system, chondroitin sulfate proteoglycans (CSPGs) have long been known as inhibitors enriched in the glial scar that prevent axon regeneration after injury. Although many studies have shown that CSPGs inhibited neurite outgrowth in vitro using different types of neurons, the mechanism by which CSPGs inhibit axonal growth remains poorly understood. Using cerebellar granule neuron (CGN) culture, in this study, we evaluated the effects of different concentrations of both immobilized and soluble CSPGs on neuronal growth, including cell adhesion, spreading and neurite growth. Neurite length decreased while CSPGs concentration arised, meanwhile, a decrease in cell density accompanied by an increase in cell aggregates formation was observed. Soluble CSPGs also showed an inhibition on neurite outgrowth, but it required a higher concentration to induce cell aggregates formation than coated CSPGs. We also found that growth cone size was significantly reduced on CSPGs and neuronal cell spreading was restrained by CSPGs, attributing to an inhibition on lamellipodial extension. The effect of CSPGs on neuron adhesion was further evidenced by interference reflection microscopy (IRM) which directly demonstrated that both CGNs and cerebral cortical neurons were more loosely adherent to a CSPG substrate. These data demonstrate that CSPGs have an effect on cell adhesion and spreading in addition to neurite outgrowth.

Key Words: chondroitin sulfate proteoglycans; cell adhesion; neurite growth; interference reflection microscopy; neural regeneration

Introduction

Being main components of extracellular matrix (ECM) in the central nervous system (CNS), chondroitin sulfate proteoglycans (CSPGs) have long been known as a class of repulsive guidance molecules during development as well as potent axon growth inhibitors after CNS injury (Miller and Hsieh-Wilson, 2015). The level of CSPGs in the CNS decreases with age, and CSPGs become concentrated into perineuronal nets, which play important roles in limiting plasticity of the adult CNS (Miyata and Kitagawa, 2016). After CNS injury, CSPGs are upregulated in the glial scar which presents a barrier to axonal regeneration. Nevertheless, the mechanism by which CSPGs inhibit axonal growth remains poorly understood. Recent experiments have identified the type IIa protein phosphatases RPTP σ and LAR, and the Nogo receptors (NgR1 and NgR3) as CSPG receptors (Shen et al., 2009; Fisher et al., 2011; Dickendesher et al., 2012; Lang et al., 2015). However, these same receptors can bind Heparan sulfate proteoglycans (HSPGs) (Aricescu et al., 2002; Fox and Zinn, 2005), which facilitate neurite outgrowth, suggesting that other mechanisms may be involved in signaling by CSPGs.

Several neuron cell culture models implicate the control of neurite outgrowth by mechanical forces (Kerstein et al., 2015). Under these models, the growth cone adheres to the substrate, and membrane proteins such as integrins form linkages between the substrate and the cytoskeleton, allowing the growth cone to extend by exerting traction forces (Athamneh and Suter, 2015). We have demonstrated that neuronal growth cones are very sensitive to substrate stiffness, with different neuronal populations being tuned to different levels of stiffness (Koch et al., 2012). One key component of this model is the role of cellular adhesion – without adhering to the substrate, neurons would not be able to exert traction forces and extend. Therefore, understanding the role of adhesion may provide important clues regarding how axonal growth is modulated.

Cell adhesion is normally regulated by the attachment of transmembrane integrins to extracellular matrix (ECM) molecules. Laminin, fibronectin, and tenascin-C bind to integrins to support cell adhesion, while the role of CSPGs in cell adhesion is not entirely clear. Proteoglycans, including CSPGs on the cell surface, can facilitate cell adhesion to other matrix proteins like fibronectin (Conget and Minguell,

*Correspondence to:

Panpan Yu, Ph.D.,
yupanpan21@jnu.edu.cn.

These authors contributed
equally to this work.

orcid:
0000-0002-4479-1479
(Panpan Yu)

doi: 10.4103/1673-5374.226398

Accepted: 2017-12-20

1994). In contrast, CSPG substrates have been shown to be anti-adhesive for several different types of cells, including fibroblasts (Knox and Wells, 1979), hepatocytes (Kato et al., 1995) and several types of neurons (Friedlander et al., 1994; Maeda and Noda, 1996). Neurons plated onto CSPG substrates adhere poorly, and neurites are often found to be fasciculated, in contrast to neurons plated on poly-L-lysine (PLL) or laminin (Maeda and Noda, 1996; Condic et al., 1999; Snow et al., 2003; Hayashi et al., 2005). This behavior has been interpreted as due to the anti-adhesive properties of CSPGs. In this work, we demonstrated the effects of CSPGs on neuronal cell attachment, spreading, neurite growth as well as growth cone morphology. We provide direct evidence that CSPGs are anti-adhesive through the use of interference reflection microscopy (IRM).

Materials and Methods

Primary neuron isolation

Mouse cerebellar granule neurons (CGNs) were isolated from postnatal 5–8 day old C57BL/6 mice. In brief, cerebella were dissected out and digested with 0.125% trypsin for 15 minutes at 37°C. After dissociation into a single cell suspension by trituration, cells were cultured in Neurobasal-A medium containing B27 (1:50, v/v) supplemented with Glutamax (Life technologies corporation, Grand Island, NY, USA) and 25 mM KCl.

Cerebral cortical neurons were isolated from E18-19 C57BL/6 mouse embryos. In brief, cortices were dissected out and digested with 0.05% trypsin (Life Technologies Corporation, Grand Island, NY, USA) for 15 minutes at 37°C. After dissociation into a single cell suspension, cells were cultured in Neurobasal medium containing B27 (1: 50, v/v) supplemented with Glutamax (Life Technologies Corporation).

All animal procedures were approved by the Laboratory Animal Ethics Committee of Jinan University and by the Institutional Animal Care and Use Committee at the National Heart, Lung, and Blood Institute of National Institutes of Health and performed in accordance with their guidelines.

Immunostaining and Imaging

To monitor changes in cell morphology on CSPGs, cells on coverslips were fixed with 4% paraformaldehyde (PFA) for 15 minutes and then stained with β -tubulin III and 4',6-diamidino-2-phenylindole (DAPI), Texas Red-Phalloidin (1:200; Molecular Probes Inc., Eugene, OR, USA) and DAPI, AlexaFluor488-Phalloidin (1:200, Molecular Probes Inc., Eugene, OR, USA) and DAPI, or with β -tubulin III, TexasRed-Phalloidin and DAPI. For F-actin staining with Phalloidin, cells were first blocked with 10% normal goat serum in phosphate buffer saline (PBS) containing 0.1% Triton X-100 (PBST) for 30 minutes at room temperature and then incubated with TexasRed-Phalloidin (1:200; Molecular Probes Inc.) or AlexaFluor488-Phalloidin (1:200; Molecular Probes Inc.) and DAPI diluted in PBST with 2.5% normal goat serum for 30 minutes at room temperature. After three washes with PBS, coverslips were mounted on slides with

aqueous gel mount. For β -tubulin III staining, cells were blocked with 10% normal goat serum in PBST for 1 hour at room temperature followed by incubation with mouse anti- β -tubulin III (1:1,000; Sigma, St. Louis, MO, USA) primary antibody diluted in PBST with 2.5% normal goat serum for 1 hour at room temperature. After three washes with PBS, cells were then incubated with AlexaFluor488-Goat anti-Mouse IgG secondary antibody (1:1,000; Life Technologies Corporation) and DAPI diluted in PBST with 2.5% normal goat serum for 1 hour at room temperature. In the case of β -tubulin III and Phalloidin costaining, Texas Red-Phalloidin (1:200; Molecular Probes Inc.) was added at the secondary antibody incubation step. Fluorescence images were captured on a Nikon E1000 upright microscope equipped with a Zeiss AxiocamHRc camera (Carl Zeiss, Thornwood, NY, USA) controlled by Zeiss Axiovision software, or on a Zeiss LSM510 or a Zeiss LSM780 confocal microscope (Carl Zeiss MicroImaging, Jena, Germany) with a 63 \times 1.4 NA oil immersion objective.

Observation of neurite outgrowth and growth cone morphology

Coverslips in 24-well plates were first coated with 200 μ g/mL poly-L-lysine (PLL) (Sigma) for 2 hours at 37°C. After three washes with sterile water, the coverslips were covered with various concentrations (0, 1, 2, 4 μ g/mL) of CSPGs (Millipore, Temecula, CA, USA) diluted in PBS and incubated at 37°C for 2 hours. After rinse with sterile PBS, dissociated CGNs were plated at a density of 1×10^4 cells/well in 1 mL of medium and cultured for 2 days. Relative neurite length was measured after staining with β -tubulin III by a stereological method (Ronn et al., 2000) using ImageJ (<https://imagej.nih.gov/ij/>) as described previously (Yu et al., 2012). The total number of DAPI-stained cells in each field and the number of aggregated cells were counted using ImageJ and the percentage of aggregated cells was calculated. For testing the effects of soluble CSPGs, various concentrations of CSPGs (0, 1, 2, 4, 10 μ g/mL) were added into the culture medium at the time of cell plating. Cells were fixed 1 or 3 days later. After staining with β -tubulin III and DAPI, neurites were traced for each individual neuron and the total neurite length and the percentage of neurons with neurites longer than two cell body sizes were measured using ImageJ. Growth cones of CGNs were visualized using β -tubulin III and Texas Red-Phalloidin staining, and the size of the growth cone after 1 day in culture was measured by tracing using ImageJ. Data were collected from three independent experiments and normalized to the PLL control group (0 μ g/mL of CSPG).

Neuronal spreading analysis

Coverslips in 24-well plates were first coated with 200 μ g/mL PLL (Sigma) for 2 hours at 37°C. After three washes with sterile water, the coverslips were coated with 1 μ g/mL of CSPGs (Millipore, Temecula, CA, USA) diluted in PBS or PBS only; alternately, the coverslips were coated with 5 μ g/mL Laminin (LN) (Thermo Fisher) with or without 1 μ g/mL CSPGs diluted

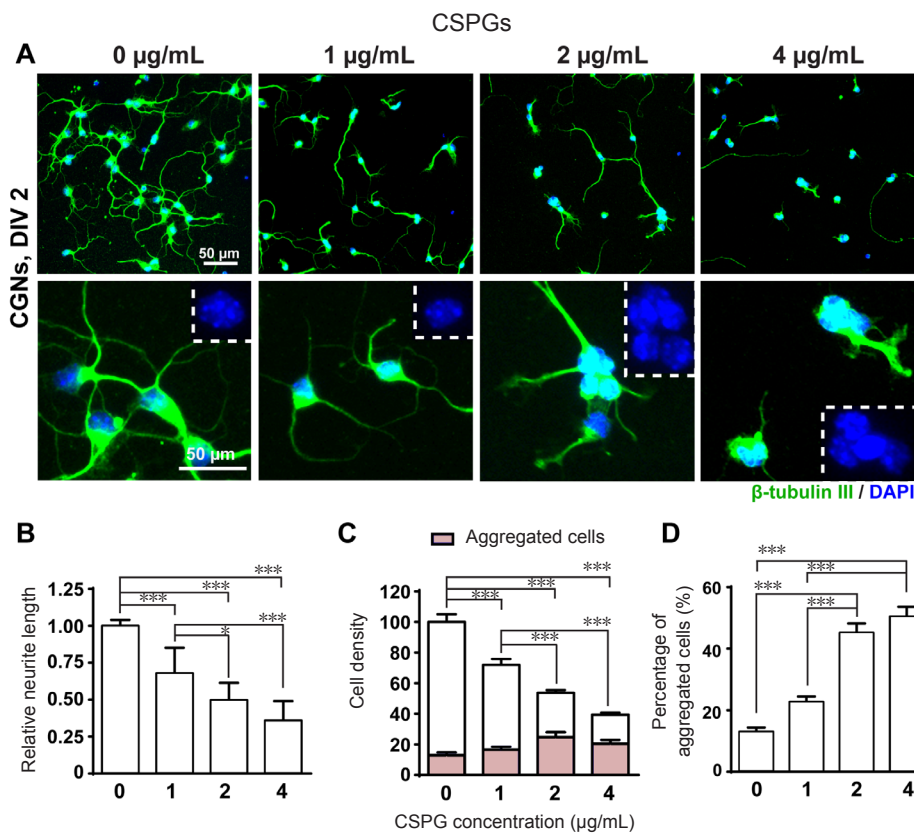


Figure 1 Effects of CSPGs coating on the growth of CGNs.

CGNs were fixed after 2 days of culture (DIV2) and stained with β -tubulin III (green) and 4',6-diamidino-2-phenylindole (DAPI; blue). (A) Representative images of CGNs growing on increasing concentrations (0, 1, 2, 4 μ g/mL) of CSPG substrates. The bottom row images are the respective higher magnification images of the top row. The inserts inside the bottom row of images are DAPI-stained nucleus, showing multiple cells aggregated together in 2 μ g/mL and 4 μ g/mL CSPGs groups. Scale bars: 50 μ m. (B) Quantification of relative neurite length. Data are normalized to no CSPGs (0 μ g/mL) control. (C) Quantification of the cell density in each field. Data are normalized to no CSPGs (0 μ g/mL) control. (D) Quantification of the percentage of the aggregated cells in each field. Data are presented as the mean \pm SEM; * P < 0.05, *** P < 0.001; one-way analysis of variance with a Tukey's *post hoc* test. CSPGs: Chondroitin sulfate proteoglycans; CGN: cerebellar granule neuron.

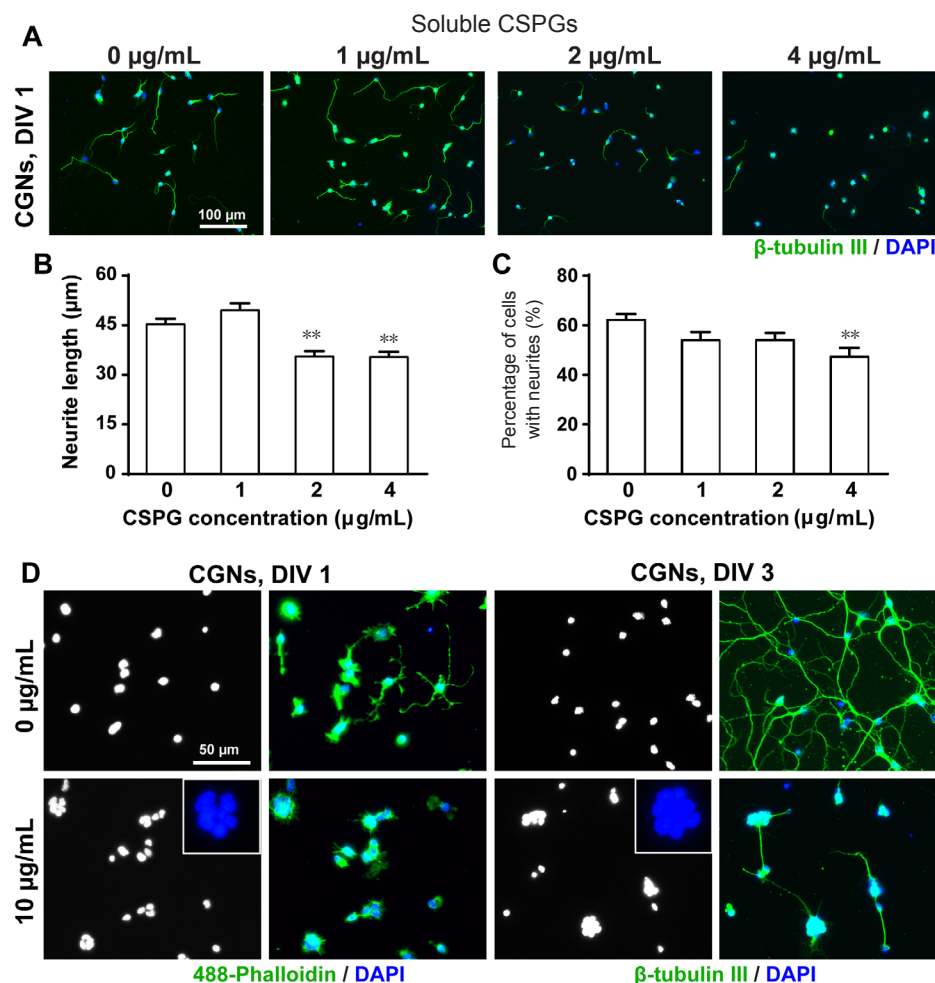


Figure 2 Effects of soluble CSPGs on the growth of CGNs.

(A) Representative images of CGNs growing on increasing concentrations of soluble CSPGs (0, 1, 2, 4 μ g/mL) for 1 day (DIV1). Neurons are stained with β -tubulin III (green) and DAPI (blue). Scale bar: 100 μ m. (B) Quantification of neurite length. (C) Quantification of the percentage of cells with neurites longer than the size of two cell bodies. (D) Representative images of CGNs growing on no CSPGs or 10 μ g/mL soluble CSPGs for 1 (DIV1) and 3 days (DIV3). CGNs fixed for 1 day were stained with 488-Phalloidin (green) and DAPI (blue). CGNs fixed for 3 days were stained with β -tubulin III (green) and DAPI (blue). Scale bar: 50 μ m. Data are presented as the mean \pm SEM; ** P < 0.01, vs. no CSPGs (0 μ g/mL) group. One-way analysis of variance (ANOVA) with a Tukey's *post hoc* test was used. CSPGs: Chondroitin sulfate proteoglycans; CGN: cerebellar granule neuron.

in PBS. Dissociated CGNs were seeded onto the coated coverslips at a density of 1×10^4 cells/well. Cells were allowed to adhere to coverslips for 30 minutes and 2 hours, and were then directly fixed with 4% PFA in the wells after gently removing culture medium without a pre-wash with PBS. Cells were stained with Texas Red-Phalloidin and DAPI. The area of individual cells at 30 minutes after plating on different substrates was measured using ImageJ. The percentage of cells with neurites longer than two cell body size was calculated at 2 hours after plating. Data were collected from three independent experiments.

Neuronal adhesion analysis using interference reflection microscopy

Cells for IRM analysis were plated on 35 mm glass-bottom dishes (MatTek, Ashland, MA, USA) pre-coated with PLL (200 $\mu\text{g}/\text{mL}$), PLL (200 $\mu\text{g}/\text{mL}$) + CSPGs (1 $\mu\text{g}/\text{mL}$), PLL + LN (5 $\mu\text{g}/\text{mL}$), PLL + LN (5 $\mu\text{g}/\text{mL}$) + CSPGs (1 $\mu\text{g}/\text{mL}$). CGNs or cortical neurons were plated at a density of 2×10^4 cells/well and then fixed with 4% PFA at 30 minutes and 2 hours after plating after gently removing the culture medium. IRM images were obtained with a Zeiss 780 LSM confocal microscope using Zeiss 63 \times 1.4 NA oil immersion objective. A 488 nm laser was used to generate a reflection image at a focal plane where the cell was attached to the glass surface. Single-frame TIFF images were processed using background subtraction and contrast increase to display areas of minimum and maximum adhesion of the cell to the glass surface using ImageJ. A color map 'Gem' was used to display higher intensity pixels as blue and lower intensity as orange which represent stronger and weaker adhesions, respectively. For quantification, the area of each cell was traced from bright field images to obtain an area ROI. A threshold was applied to the IRM image of the same cell and the number of pixels above threshold was divided by the area of the region of interest (ROI) to calculate the percentage of adhesion.

Statistical analysis

Statistical analyses were performed either by one-way analysis of variance (ANOVA) with Tukey's *post hoc* test or by a two-tailed Student's *t*-test using GraphPad Prism (GraphPad, San Diego, CA, USA). Results were considered statistically significant if $P < 0.05$.

Results

CGNs tended to form aggregates in the presence of increasing concentrations of CSPGs

Our initial objective was to create a dose-response curve for the inhibitory effect of CSPGs on neurite outgrowth. When CGNs were plated on substrates of PLL plus different concentrations (0, 1, 2, 4 $\mu\text{g}/\text{mL}$) of CSPGs, the total neurite length decreased as a function of CSPG concentration (Figure 1A, B). At the same time, we observed a decrease in cell density accompanied by an increase in the formation of cell aggregates with increasing CSPG concentration. The average cell number per field was significantly reduced in the 1 $\mu\text{g}/\text{mL}$ CSPG-coated group, and was further decreased

in the 2 $\mu\text{g}/\text{mL}$ CSPG-coated group, and became less than a half in the 4 $\mu\text{g}/\text{mL}$ CSPG-coated group (Figure 1C). While the number of cells per field decreased with CSPG concentration, we also observed that neurons growing on CSPGs substrates tended to form aggregates (Figure 1D). Nearly 50% of the neurons in 2 and 4 $\mu\text{g}/\text{mL}$ CSPG-coating groups were aggregated, and neurites extending from the aggregates were often fasciculated, which was consistent with previous findings (Snow et al., 2003). Notably, we found that the activity of CSPGs obtained commercially varies from batch to batch, and therefore optimization of concentrations is required for each new batch of CSPGs.

There is evidence that neurons respond differently to substratum-bound CSPGs versus soluble CSPGs (Snow et al., 1996). We next examined whether soluble CSPGs also show a similar effect on CGN adhesion. CSPGs (1, 2, 4 $\mu\text{g}/\text{mL}$) were added into the culture medium at the time of cell plating. Neurite outgrowth was also inhibited by the addition of soluble CSPGs at 2 and 4 $\mu\text{g}/\text{mL}$ concentrations and the number of neurite-bearing cells significantly reduced at 4 $\mu\text{g}/\text{mL}$ (Figure 2A–C).

Considering the local CSPGs concentration might be much higher when CSPGs were applied as a coating substrate as compared to the same concentration of the soluble form added into culture medium, we then increased the concentration of soluble CSPGs up to 10 $\mu\text{g}/\text{mL}$. This concentration significantly inhibited the outgrowth of neurites and increased the formation of cell aggregates on day 1. By 3 days, in the control group, neurites extending from individual isolated neurons formed a network with each other; however, in the 10 $\mu\text{g}/\text{mL}$ CSPG-treated group, only a few short fasciculated neurites extended out from cell aggregates (Figure 2D). Thus, soluble CSPGs showed a comparable effect to that on a substrate, but required a higher concentration as compared to substratum-bound CSPGs.

CSPGs reduced the size of growth cone of CGNs by limiting lamellipodia formation

Neurite elongation and guidance are under the control of growth cone located at the distal tip of an advancing neurite. Driven by polymerization and depolymerization of actin filaments, growth cones constantly protrude and withdraw filopodia and lamellipodia from its leading margin, in response to extrinsic adhesive ligands or soluble guidance cues (Dent and Gertler, 2003; Gomez and Letourneau, 2014). We therefore sought to examine the morphological changes of growth cone. In CGNs growing on PLL, a typical growth cone was present at the axon tip, which was composed of a central domain and a peripheral domain with filopodia and lamellipodia formed at the leading edge. In contrast, growth cones in the CSPGs group often had numerous filopodia but contained small lamellipodial veils (Figure 3A). At 1 $\mu\text{g}/\text{mL}$ CSPG coating, the size of growth cone was significantly reduced as compared to that in the PLL group (Figure 3B). This is likely attributed to the small lamellipodial size in the peripheral domain, suggesting that CSPGs inhibited growth cone spreading by limiting lamellipodia extension at the

leading edge.

CSPGs affected CGNs spreading by limiting lamellipodia formation at early time point after plating

To further illustrate the influence of CSPGs on neuronal morphology, we looked at the spreading of neuronal soma shortly after cell plating. CGNs growing on PLL displayed a pancake shape at 30 minutes after plating by spreading out lamellipodia. However, cells on CSPGs remained as spherical shapes with restrained lamellipodia extension. A 3D reconstruction also demonstrated that neurons plated on PLL had a much wider base than that on CSPGs (**Figure 4A and B**). To our surprise, CGNs plated on laminin (LN) also showed a spherical shape with restrained spreading, morphologically similar to those growing on CSPGs (**Figure 4A**). The cell spreading areas in the PLL + CSPGs and PLL + LN groups were significantly reduced as compared to the areas of neurons plated on PLL, and it was further reduced for neurons plated on the mixture of PLL + LN + CSPGs (**Figure 4C**).

At 2 hours after plating, CGNs on PLL underwent a cell shape switch by extending out several tiny protrusions (filopodia); some cells started the initiation of neurites but only a very few had neurite lengths longer than two cell body sizes (**Figure 4D and E**). In contrast, an increased number of neurons extended neurites longer than two cell body sizes on LN (**Figure 4D and F**), confirming a neurite growth promoting effect of LN. When plated on CSPGs, very few cells extended neurites at 2 hours after plating, no matter whether there was LN or not (**Figure 4D and F**). After 1 day of culture, the length of neurites growing on LN plus CSPGs was only about one third of the length of those growing on LN (**Figure 5**). The differences between LN and LN + CSPG seemed more prominent than the differences between PLL and PLL + CSPGs (**Figures 1, 2**). This indicates that the presence of growth promoting LN was not sufficient to overcome or neutralize the inhibitory effect of CSPGs.

CSPGs affected neuronal cell adhesion both on PLL and LN

Both LN and CSPGs showed an inhibition of cell spreading as compared to PLL, despite their opposite effects on neurite initiation. We next sought to measure cell adhesion status using IRM. IRM is an optical technique that generates images based on interference between reflected light from the glass surface of a coverslip and the cell membrane. Closer distances causing more interference with darker pixels, and further distances have less interference with lighter pixels. Furthermore, it enables visualization of very fine cell contours attached to a glass substrate. We examined CGN and cortical neuron attachment to glass coverslips coated with PLL, PLL + CSPG, PLL + LN, PLL + LN + CSPG at 30 minutes and 2 hours after plating. The acquired IRM images were processed to subtract background and the darker contrast areas represent higher contact between cells and coverslip. At 30 minutes after plating on PLL, CGNs and cortical neurons underwent cell spreading process, the base of the cell body already had a high degree of attachment. While on the PLL + LN, although neurons showed a lower

degree of cell spreading, the degree of cell adhesion detected by IRM was comparable to PLL. The opposite was seen on PLL + CSPG coating where most of the cells were not attached and a few were loosely attached to the coverslip at 30 minutes after plating. The addition of LN showed little effect on facilitating cell adhesion to CSPGs, as neurons on PLL + LN + CSPG displayed no better attachment than on PLL + CSPG (**Figure 6A**). At 2 hours after plating, the cell morphology showed little change on PLL compared to 30 minutes time point, and neurons maintained a firm adhesion to PLL. Neurons on the PLL + CSPG were still loosely attached to the coverslips with light pixels detected by IRM. Dark pixels were obtained again in CGNs and cortical neurons on the PLL + LN substrates at 2 hours after plating and neurons started extending neurites from their cell bodies. However, neurons on the PLL + LN + CSPG substrates still had very weak attachment to the coverslips (**Figure 6B**).

Discussion

CSPGs are long known for their ability to inhibit neurite outgrowth in culture. Herein we demonstrate this ability through the use of cultures of CGNs. Increasing concentrations of CSPGs inhibited neurite outgrowth, when applied as either a substrate or in solution. Moreover, when plated onto CSPGs, neuronal somas aggregate and neurites were fasciculated. Freshly plated neurons spread on the PLL rapidly, yet this spreading was inhibited on a combination of PLL and CSPGs. IRM directly demonstrated that the CSPG substrate inhibited neuronal adhesion. Taken together, these data clearly demonstrate that CSPGs have a negative effect on cell adhesion in addition to inhibition of neurite outgrowth.

Surface wettability is normally measured by the contact angle of a water droplet, the lower the contact angle, the more wettable the surface. Wettability is determined by the balance of cohesive forces in a liquid and adhesion to the substrate. Using 3D reconstruction of the confocal images of individual cells, we found that neurons plated on different substrates behaved similarly to water droplets, with neurons on PLL having a lower contact angle than neurons plated on either CSPGs or laminin.

In IRM, part of a cell close to the surface of a coverslip is dark because of the interference of reflected light from the surface of the coverslip and the cell, while the regions further away are either grey or, if far enough away, white (Izzard and Lochner, 1976, 1980). Dark areas are then interpreted as being ones of high adhesion, while the lighter areas have lower adhesion. IRM of growth cones was first investigated by Letourneau (1979) who reported that chick dorsal root ganglion neurons plated on uncoated glass did not show close apposition to the coverslip, while those plated on PLL-coated glass did. These studies were extended to ECM substrates by Gundersen (1988) who found neuronal growth cones on LN and PLL have overall decreased growth cone-substrate association compared to those on collagen and fibronectin. Our IRM results measured from freshly-plated neurons demonstrate a high degree of adhesion

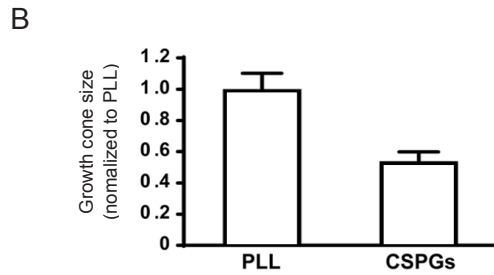
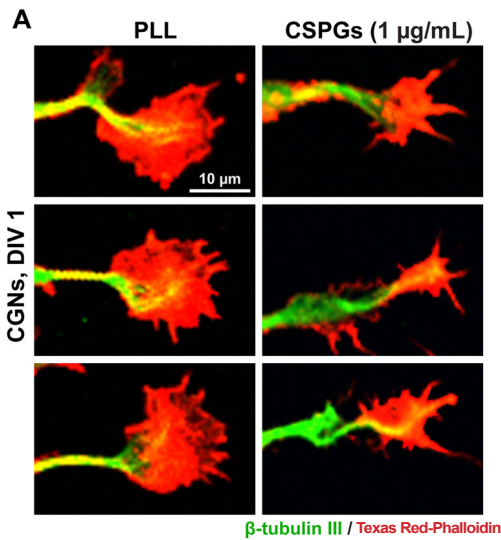


Figure 3 Effect of CSPGs on the morphology of growth cone.

(A) Representative images showing the morphology of growth cones of CGNs growing on PLL for 1 day (DIV1) with or without 1 µg/mL CSPGs. Neurons are stained with β -tubulin III (green) and Texas Red-Phalloidin (red). Scale bar: 10 µm. (B) Quantification of the growth cone size. Data are presented as the mean \pm SEM; $**P < 0.01$. Two-tailed Student's *t*-test was used. CSPGs: Chondroitin sulfate proteoglycans; CGNs: cerebellar granule neurons; PLL: poly-L-lysine.

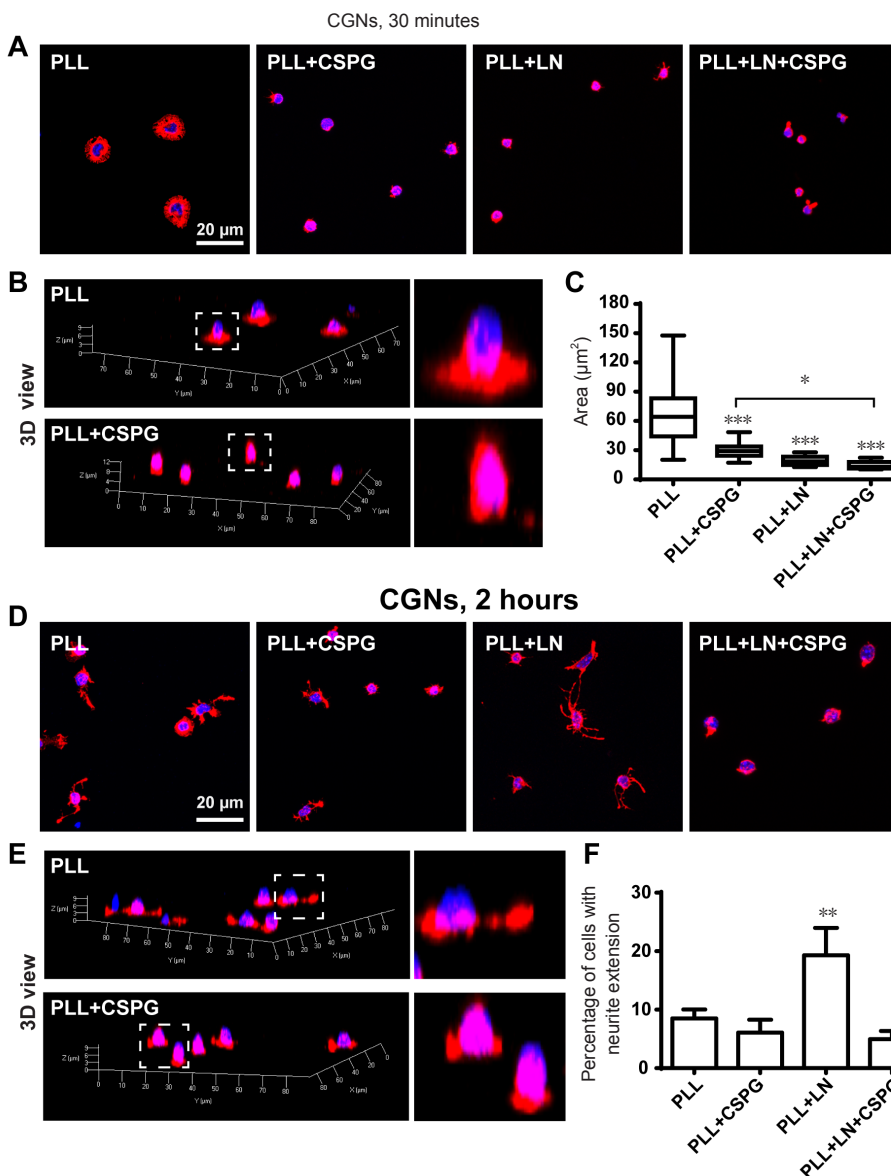


Figure 4 Effects of CSPGs on neuronal spreading and neurite initiation with or without the presence of LN.

(A) Neuron spreading status at 30 minutes after plating on PLL, PLL + CSPGs (1 µg/mL), PLL + LN, or PLL + LN + CSPGs (1 µg/mL). Scale bar: 20 µm. (B) Three-dimensional demonstration of the overall morphology of neurons on PLL and PLL + CSPGs at 30 minutes after plating. (C) Quantification of neuronal spreading area. Data are presented as the mean \pm SEM; $***P < 0.001$, vs. PLL group; $*P < 0.05$ for comparison between PLL + CSPG and PLL + LN + CSPG; one-way analysis of variance with a Tukey's *post hoc* test was used. (D) Neuronal morphology at 2 hours after plating on PLL, PLL + CSPGs, PLL + LN, or PLL + LN + CSPGs. Scale bar: 20 µm. (E) Three-dimensional manifestation of the overall morphology of neurons on PLL and PLL + CSPGs at 2 hours after plating. (F) Quantification of the percentage of neurons with neurite initiation. Data are presented as the mean \pm SEM; $**P < 0.01$, vs. PLL, PLL + CSPG, or PLL + LN + CSPG; one-way analysis of variance with a Tukey's *post hoc* test was used. CGNs: Cerebellar granule neurons; CSPGs: chondroitin sulfate proteoglycans; LN: laminin; PLL: poly-L-lysine.

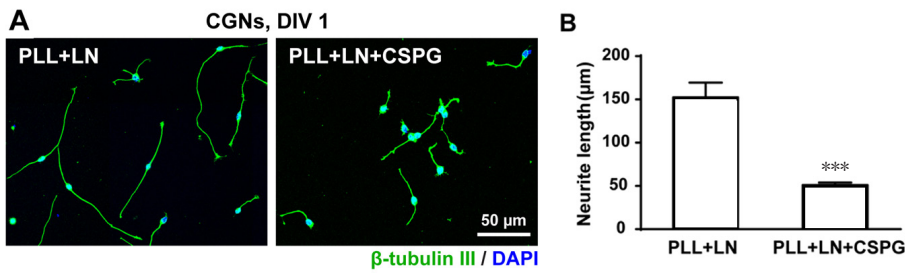


Figure 5 CSPGs showed a prominent inhibition on neurite outgrowth in the presence of LN.

(A) Representative images of CGNs growing on PLL + LN and PLL + LN + CSPGs (1 µg/mL) for 1 day (DIV1). Neurons are stained with β-tubulin III (green) and DAPI (blue). Scale bar: 50 µm. (B) Quantification of neurite length. Data are presented as the mean ± SEM; *** $P < 0.001$; two-tailed Student's t -test. CGNs: Cerebellar granule neurons; CSPGs: chondroitin sulfate proteoglycans; LN: laminin; DAPI: 4',6-diamidino-2-phenylindole.

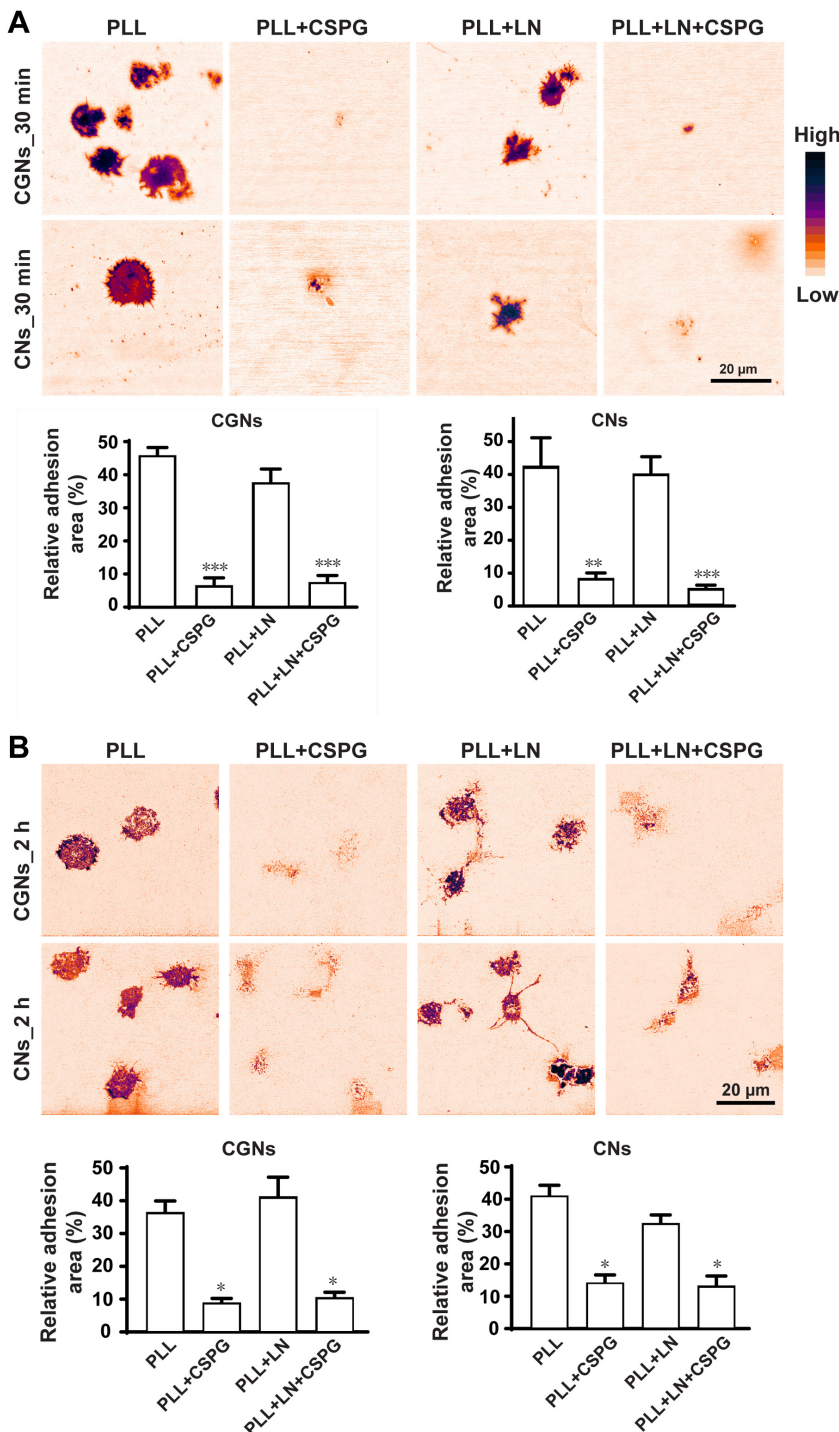


Figure 6 IRM results showing the anti-adhesive effect of CSPGs.

(A) Representative IRM images and quantifications of CGNs and cerebral cortical neurons (CNs) growing on PLL, PLL + CSPGs (1 µg/mL), PLL + LN and PLL + LN + CSPGs (1 µg/mL) for 30 minutes. (B) Representative IRM images and quantifications of CGNs and cerebral cortical neurons (CNs) growing on the PLL, PLL + CSPGs (1 µg/mL), PLL + LN and PLL + LN + CSPGs (1 µg/mL) for 2 hours. Single-frame TIFF images of IRM were processed to display areas of minimum and maximum adhesion of the cells to the glass surface. Images were processed for background subtraction and color map named 'Gem' was assigned blue to higher intensity and orange to lower intensity pixels which represent stronger and weaker adhesions respectively. Area of the cell was traced using the bright field images to obtain "ROI". The ROI was placed on the binary processed IRM image and the percentage of adhesion (relative adhesion area) was calculated by dividing the area of the cell by the area of adhesion. Cell adhesion of CGNs or cortical neurons was significantly reduced on the PLL + CSPG or PLL + LN + CSPG substrates compared to that on the PLL or PLL + LN substrate. Data are presented as the mean ± SEM; * $P < 0.05$, ** $P < 0.01$, *** $P < 0.001$, one-way analysis of variance with a Tukey's *post hoc* test was used. Scale bars: 20 µm. IRM: Interference reflection microscopy; CSPGs: chondroitin sulfate proteoglycans; CGNs: Cerebellar granule neurons; PLL: poly-L-lysine; LN: laminin.

both on the LN and PLL substrate, despite a more restrained soma spreading observed on LN compared to PLL. Moreover, we show that adhesion is further reduced when neurons are plated on CSPGs. Collectively, neurons on PLL adhere firmly and display a high extent of cell spreading with a low contact angle; neurons on LN adhere tightly although show a restrained spreading with a high contact angle; while neurons on CSPGs show both a poor adhesion and spreading.

Given the facts that CSPGs inhibit neurite generation, while neurons on LN rapidly grow neurites as compared to PLL, our data implicate that: 1) a high degree of cell spreading in some extent might restrain neurite initiation; 2) a low degree of cell spreading but with a tight attachment would facilitate neurite initiation; 3) a low degree of cell spreading with a loose attachment is certainly not optimal for neurite generation and stabilization. These results would confirm that, unlike PLL, CSPGs are anti-adhesive and limit cell spreading. In terms of LN, although it restrained cell spreading, it provided an adequate degree of neuron-substrate association for neurite initiation.

Laminins engage integrins, while CSPGs do not. In fact, evidence suggests that CSPGs interfere with integrin-mediated adhesion (Iida et al., 1992). Neurotrophins support regenerative axon assembly over CSPGs by an ECM-integrin-independent mechanism (Zhou et al., 2006). In contrast, integrins are the major receptors for laminin-mediated neurite outgrowth (Tomaselli et al., 1993). Others have shown that neurons growing on CSPGs upregulate their integrin receptors (Condic et al., 1999), that activating integrins may overcome CSPG inhibition in culture (Tan et al., 2011), and that expression of integrins can promote long-distance regeneration after spinal cord injury (Cheah et al., 2016). However, a combination of laminin and CSPGs did not promote neurite outgrowth in our experiments. It may be that the time period was too short for integrins to be upregulated, CSPGs masked the integrin interactions, or CGNs, unlike dorsal root ganglion neurons, do not upregulate their integrins in response to CSPGs.

Neurites from neurons growing on CSPGs displayed a large degree of fasciculation. This has been previously observed (Snow et al., 2003), and was attributed to poor adhesion. However, many different factors control fasciculation, such as the homophilic interactions of cell adhesion molecules and cadherins (Drazba and Lemmon, 1990; Honig et al., 1998). Lemmon et al. (1992) examined fasciculation as well as growth of retinal ganglion neurites, and also measured relative adhesion of growth cones. Their conclusion was that there was a poor correlation between growth rate, fasciculation, and adhesion. Another conclusion can also be drawn from their analysis that the two most adhesive substrates generated the slowest growth rate, which may be interpreted as that excess adhesion cannot be overcome by force generation. We also observed a bell-shaped curve for neurite outgrowth on the substrates of different stiffness (Koch et al., 2012). Taken together, these data and our current data suggest that there is an optimum degree of adhesion and spreading to promote neurite outgrowth in culture.

In summary, control of neurite outgrowth is a multifarious process involving many different parameters. We demonstrate that CSPGs inhibit neurite outgrowth in a dose-dependent fashion. We also confirmed that CSPGs are anti-adhesive. Moreover, neurons on LN and PLL have a similar extent of adhesion, but neurons on LN display a more restrained spreading than PLL, which promotes neurite outgrowth. We propose that especially at the higher concentrations of CSPG, the reduced neurite outgrowth results from both a direct inhibition of CSPGs on neurite extension and a poor adhesion, which hence affect neurite extension or stabilization.

Author contributions: PY conceived and designed the study. PY, JJ and ST conducted the experiments and analyzed the data. ZH participated in data collection and analysis. HMG and LZ contributed to the conception and design of this study. LZ provided technical assistance. The paper was written by PY and HMG with contributions from all authors. All authors approved the final version of this paper.

Conflicts of interest: The authors declare no competing financial interests.
Financial support: This work was supported by the National Natural Science Foundation of China, No. 81601066; the National Science Foundation of Guangdong Province of China, No. 2017A030313103 and 2016A030313096; a grant from the Program of Introducing Talents of Discipline to Universities, No. B14036; the Fundamental Research Funds for the Central Universities, No. 21616340; and the Division of Intramural Research of the National Heart, Lung, and Blood Institute of National Institutes of Health. The funding bodies played no role in the study design, in the collection, analysis and interpretation of data, in the writing of the paper, and in the decision to submit the paper for publication.

Research ethics: All animal procedures were approved by the Laboratory Animal Ethics Committee of Jinan University and by the Institutional Animal Care and Use Committee at the National Heart, Lung, and Blood Institute of National Institutes of Health of USA and performed in accordance with their guidelines.

Data sharing statement: Datasets analyzed during the current study are available from the corresponding author on reasonable request.

Plagiarism check: Checked twice by iThenticate.

Peer review: Externally peer reviewed.

Open access statement: This is an open access article distributed under the terms of the Creative Commons Attribution-NonCommercial-ShareAlike 3.0 License, which allows others to remix, tweak, and build upon the work non-commercially, as long as the author is credited and the new creations are licensed under identical terms.

References

- Aricescu AR, McKinnell IW, Halfter W, Stoker AW (2002) Heparan sulfate proteoglycans are ligands for receptor protein tyrosine phosphatase sigma. *Mol Cell Biol* 22:1881-1892.
- Athamneh AI, Suter DM (2015) Quantifying mechanical force in axonal growth and guidance. *Front Cell Neurosci* 9:359.
- Cheah M, Andrews MR, Chew DJ, Moloney EB, Verhaagen J, Fassler R, Fawcett JW (2016) Expression of an activated integrin promotes long-distance sensory axon regeneration in the spinal cord. *J Neurosci* 36:7283-7297.
- Condic ML, Snow DM, Letourneau PC (1999) Embryonic neurons adapt to the inhibitory proteoglycan aggrecan by increasing integrin expression. *J Neurosci* 19:10036-10043.
- Conget P, Minguell JJ (1994) Modifications in the synthesis of membrane-associated chondroitin sulfate proteoglycans in hemopoietic progenitor cells are accompanied by alterations in their adhesive properties. *J Cell Physiol* 159:142-150.
- Dent EW, Gertler FB (2003) Cytoskeletal dynamics and transport in growth cone motility and axon guidance. *Neuron* 40:209-227.
- Dickendeshler TL, Baldwin KT, Mironova YA, Koriyama Y, Raiker SJ, Askew KL, Wood A, Geoffroy CG, Zheng B, Liepmann CD, Katagiri Y, Benowitz LI, Geller HM, Giger RJ (2012) NgR1 and NgR3 are receptors for chondroitin sulfate proteoglycans. *Nat Neurosci* 15:703-712.

- Drazba J, Lemmon V (1990) The role of cell adhesion molecules in neurite outgrowth on Muller cells. *Dev Biol* 138:82-93.
- Fisher D, Xing B, Dill J, Li H, Hoang HH, Zhao Z, Yang XL, Bachoo R, Cannon S, Longo FM, Sheng M, Silver J, Li S (2011) Leukocyte common antigen-related phosphatase is a functional receptor for chondroitin sulfate proteoglycan axon growth inhibitors. *J Neurosci* 31:14051-14066.
- Fox AN, Zinn K (2005) The heparan sulfate proteoglycan syndecan is an in vivo ligand for the Drosophila LAR receptor tyrosine phosphatase. *Curr Biol* 15:1701-1711.
- Friedlander DR, Milev P, Karthikeyan L, Margolis RK, Margolis RU, Grumet M (1994) The neuronal chondroitin sulfate proteoglycan neurocan binds to the neural cell adhesion molecules Ng-CAM/L1/NILE and N-CAM, and inhibits neuronal adhesion and neurite outgrowth. *J Cell Biol* 125:669-680.
- Gomez TM, Letourneau PC (2014) Actin dynamics in growth cone motility and navigation. *J Neurochem* 129:221-234.
- Gundersen RW (1988) Interference reflection microscopic study of dorsal root growth cones on different substrates: assessment of growth cone-substrate contacts. *J Neurosci Res* 21:298-306.
- Hayashi N, Mizusaki MJ, Kamei K, Harada S, Miyata S (2005) Chondroitin sulfate proteoglycan phosphacan associates with parallel fibers and modulates axonal extension and fasciculation of cerebellar granule cells. *Mol Cell Neurosci* 30:364-377.
- Honig MG, Petersen GG, Rutishauser US, Camilli SJ (1998) In vitro studies of growth cone behavior support a role for fasciculation mediated by cell adhesion molecules in sensory axon guidance during development. *Dev Biol* 204:317-326.
- Iida J, Skubitz AP, Furcht LT, Wayner EA, McCarthy JB (1992) Coordinate role for cell surface chondroitin sulfate proteoglycan and alpha 4 beta 1 integrin in mediating melanoma cell adhesion to fibronectin. *J Cell Biol* 118:431-444.
- Izzard CS, Lochner LR (1976) Cell-to-substrate contacts in living fibroblasts: an interference reflexion study with an evaluation of the technique. *J Cell Sci* 21:129-159.
- Izzard CS, Lochner LR (1980) Formation of cell-to-substrate contacts during fibroblast motility: an interference-reflexion study. *J Cell Sci* 42:81-116.
- Kato S, Sugiura N, Kimata K, Kujiraoka T, Toyoda J, Akamatsu N (1995) Chondroitin sulfate immobilized onto culture substrates modulates DNA synthesis, tyrosine aminotransferase induction, and intercellular communication in primary rat hepatocytes. *Cell Struct Funct* 20:199-209.
- Kerstein PC, Nichol RI, Gomez TM (2015) Mechanochemical regulation of growth cone motility. *Front Cell Neurosci* 9:244.
- Knox P, Wells P (1979) Cell adhesion and proteoglycans. I. The effect of exogenous proteoglycans on the attachment of chick embryo fibroblasts to tissue culture plastic and collagen. *J Cell Sci* 40:77-88.
- Koch D, Rosoff WJ, Jiang J, Geller HM, Urbach JS (2012) Strength in the periphery: growth cone biomechanics and substrate rigidity response in peripheral and central nervous system neurons. *Biophys J* 102:452-460.
- Lang BT, Cregg JM, DePaul MA, Tran AP, Xu K, Dyck SM, Madalena KM, Brown BP, Weng YL, Li S, Karimi-Abdolrezaee S, Busch SA, Shen Y, Silver J (2015) Modulation of the proteoglycan receptor PTPsigma promotes recovery after spinal cord injury. *Nature* 518:404-408.
- Lemmon V, Burden SM, Payne HR, Elmslie GJ, Hlavin ML (1992) Neurite growth on different substrates: permissive versus instructive influences and the role of adhesive strength. *J Neurosci* 12:818-826.
- Letourneau PC (1979) Cell-substratum adhesion of neurite growth cones, and its role in neurite elongation. *Exp Cell Res* 124:127-138.
- Maeda N, Noda M (1996) 6B4 proteoglycan/phosphacan is a repulsive substratum but promotes morphological differentiation of cortical neurons. *Development* 122:647-658.
- Miller GM, Hsieh-Wilson LC (2015) Sugar-dependent modulation of neuronal development, regeneration, and plasticity by chondroitin sulfate proteoglycans. *Exp Neurol* 274:115-125.
- Miyata S, Kitagawa H (2016) Chondroitin sulfate and neuronal disorders. *Front Biosci* 21:1330-1340.
- Ronn LC, Ralets I, Hartz BP, Bech M, Berezin A, Berezin V, Moller A, Bock E (2000) A simple procedure for quantification of neurite outgrowth based on stereological principles. *J Neurosci Methods* 100:25-32.
- Shen Y, Tenney AP, Busch SA, Horn KP, Cuascut FX, Liu K, He Z, Silver J, Flanagan JG (2009) PTPsigma is a receptor for chondroitin sulfate proteoglycan, an inhibitor of neural regeneration. *Science* 326:592-596.
- Snow DM, Brown EM, Letourneau PC (1996) Growth cone behavior in the presence of soluble chondroitin sulfate proteoglycan (CSPG), compared to behavior on CSPG bound to laminin or fibronectin. *Int J Dev Neurosci* 14:331-349.
- Snow DM, Smith JD, Cunningham AT, McFarlin J, Goshorn EC (2003) Neurite elongation on chondroitin sulfate proteoglycans is characterized by axonal fasciculation. *Exp Neurol* 182:310-321.
- Tan CL, Kwok JC, Patani R, Ffrench-Constant C, Chandran S, Fawcett JW (2011) Integrin activation promotes axon growth on inhibitory chondroitin sulfate proteoglycans by enhancing integrin signaling. *J Neurosci* 31:6289-6295.
- Tomaselli KJ, Doherty P, Emmett CJ, Damsky CH, Walsh FS, Reichardt LF (1993) Expression of beta 1 integrins in sensory neurons of the dorsal root ganglion and their functions in neurite outgrowth on two laminin isoforms. *J Neurosci* 13:4880-4888.
- Yu P, Santiago LY, Katagiri Y, Geller HM (2012) Myosin II activity regulates neurite outgrowth and guidance in response to chondroitin sulfate proteoglycans. *J Neurochem* 120:1117-1128.
- Zhou FQ, Walzer M, Wu YH, Zhou J, Dedhar S, Snider WD (2006) Neurotrophins support regenerative axon assembly over CSPGs by an ECM-integrin-independent mechanism. *J Cell Sci* 119:2787-2796.

(Copyedited by Li CH, Song LP, Zhao M)